BMC Microbiology

RESEARCH Open Access

Transcriptomic and metabolomic analysis of the antibacterial mechanism of sanguinarine against *Enterobacter cloacae* in vitro

Ting Yang[1], Haojie Sha[1], Wenlu Bi[1], Jianguo Zeng[2] and Dingding Su[1,3*]

Abstract

Background *Enterobacter cloacae* (*E. cloacae*) is a notorious pathogen that poses serious threat to both human and animal health, causing severe gut infections and contributing to food spoilage. Traditional chemical treatment have led to increased drug resistance and environmental pollution. This study investigates the potential of Sanguinarine (SAN), a natural plant extract, as an alternative to chemical antibiotics.

Results In light of the escalating issue of antibiotic resistance, we examined the antibacterial efficacy and mechanisms of SAN against *E. cloacae in vitro*. Our findings revealed a minimum inhibitory concentration (MIC) of 100 μg/mL for SAN. Scanning electron microscopy (SEM) demonstrated substantial morphological disruptions in *E. cloacae* cells treated with SAN. Concurrently, a significant increase in absorbance at 260 nm suggested nucleic acid leakage, indicative of compromised cell membrane integrity. Comprehensive transcriptomic and metabolomic analyses revealed that SAN primarily disrupts amino acid synthesis and energy metabolism pathway in *E. cloacae*.

Conclusions SAN exhibited potential antibacterial activity against *E. cloacae*, which can effectively inhibit its growth and disrupt its bacterial morphology and exert antibacterial effect through multiple pathways, and can be used as a potential substitute for antibiotics.

Keywords *Enterobacter cloacae*, Sanguinarine, Transcriptomics, Metabolomics, Antimicrobial mechanism

Introduction

Enterobacter cloacae (*E. cloacae*) is a Gram-negative, short rod-shaped bacterium that is widespread in the environment, found in human and animal feces, soil, and plants, and is categorized as one of the normal intestinal bacteria [1]. As a pathogen in the gut of various animals, *E. cloacae* is capable of causing foodborne illnesses in humans and has been designated as a hygiene detection indicator in the food processing industry due to its association with food spoilage and contamination [2]. *E. cloacae* has been also linked to multiple diseases in humans and animals, including urinary and respiratory

*Correspondence:
Dingding Su
dingding.su@pku-iaas.edu.cn
[1]Peking University Institute of Advanced Agricultural Sciences, Weifang 262113, China
[2]Hunan Agricultural University, Changsha 410128, China
[3]Peking University Institute of Advanced Agricultural Sciences, Shandong Laboratory of Advanced Agricultural Sciences in Weifang, Weifang, Shandong 261325, China

tract infections, skin and soft tissue degeneration, and central nervous system disorders [3]. Recent studies have highlighted its role as a direct cause of obesity, indicating it significance in metabolic disorders [2]. The increasing incidence of bacterial infections caused by *E. cloacae*, often involving multiple organs, presents a significant clinical challenge due to its high resistance to many antibiotics [4]. This resistance is attributed to the production of various β-lactamases, cephalosporinases, and carbapenemases, making it difficult to treat effectively [5, 6].

Given the risk of resistance, the pursuit of novel antimicrobial agents is of critical importance. Natural plant extracts have shown considerable antibacterial properties, offering distinct advantages such as abundant availability, low incidence of adverse reactions, and a reduced likelihood for inducing drug resistance, emphasizing their unique benefits [7]. Sanguinarine (SAN), a naturally occurring benzophenanthridine alkaloid found abundantly in *Macleaya cordata (Willd.) R. Br.*, exhibits a range of biological activities, including antioxidant, antitumor, antiparasitic, anti-inflammatory, and antimicrobial effects [8]. SAN, along with its natural plant sources, has demonstrated both antimicrobial and anti-inflammatory properties, leading to its widespread use in the food and medical industries [9]. Due to its potential antimicrobial activity, SAN is commonly utilized to protect farmed fish from pathogens [10]. Additionally, it is utilized as an animal feed additive in livestock farming to enhance the intestinal flora and increase production efficiency in laying hens [11].

The study aims to investigate the bactericidal effect of SAN on *E. cloacae* and elucidate its underlying mechanism. Using scanning electron microscope, we observed morphologyical changes in cells of *E. cloacae* upon treatment with SAN. Additionally, absorbance measurements at 260 nm were utilized to assess the impact of SAN on bacterial cell membrane integrity. Comprehensive transcriptomic and metabolomic analyses were performed to unvocer the potential inhibitory mechanisms of SAN against *E. cloacae*, providing valuable insights into its antimicrobial action.

Materials and methods

Culture of *E. cloacae*

E. cloacae was purchased from Beijing Solaibao Technology Co., Ltd. *E. cloacae* was inoculated in Trypticase Soy Broth (TSB) (Qingdao Hope Bio-Technology Co., Ltd.) and cultured to the logarithmic growth phase. The bacteria were then isolated by streaking on Tryptic Soy Agar Medium (TSA) (Qingdao Hope Bio-Technology Co., Ltd.) plates. After an overnight incubation at 37°C, a typical single colony was selected and inoculated into 5 mL of fresh TSB medium. The suspension, containing 40% glycerol, was prepared by oscillating the culture overnight at 37°C and 200 r/min. The suspension was subsequently frozen at -40°C for storage. Prior to each experiment, 2% of the frozen bacterial suspension was inoculated into 5 mL of fresh TSB medium and activated by incubation for 12 h at 37°C and 200 r/min.

Preparation of SAN solution

Eight mg of SAN (Hunan Mekeda Biological Resources Co., Ltd.) was weighed and dissolved in 1 mL of dimethyl sulfoxide (DMSO) to obtain a stock solution with a concentration of 8 mg/mL. In subsequent experiments, SAN was diluted to 50, 100, 200, 400, and 800 μg/mL, respectively. The highest concentration of DMSO was 0.1%.

Inhibitory effect of SAN on the growth of *E. cloacae*

The antagonistic effect of SAN on the growth of *E. cloacae* was determined by the filter paper diffusion method [12]. Briefly, TSA plates were initially coated with 50 μL of an *E. cloacae* suspension, containing approximately 10^8 CFU/mL. Sterile filter paper disks, each containing 10 μL of SAN at different concentrations, were then placed on the surface of the agar plates. The petri dishes were sealed with parafilm and incubated at 37°C for 24 h. After incubation, the diameters of the inhibition zones were measured in millimeters, serving as indicators of the antibacterial effect of SAN. Larger inhibition zones suggested a more potent inhibitory effect of SAN against *E. cloacae*. The medium without SAN was used as a blank control, and 0.1% DMSO was used as a negative control.

Determination of MIC of SAN against *E. cloacae*

The MIC of SAN against *E. cloacae* was determined by Gutierrez-Pacheco et al. method and modified [13]. The *E. cloacae* were grown to the logarithmic phase, the optical density (OD_{600}) measured by Ultraviolet-visible Spectrophotometer (X-8, Shanghai Metash Instruments Co., Ltd, China) was 0.6. Each SAN concentration was inoculated with 2% of the bacterial culture and incubated at 37°C for 24 h, after which the samples was determined at 600 nm. In the previous experiments, 0.1% DMSO was not toxic to *E. cloacae*. Therefore, the medium without SAN was selected as the control. The MIC was identified as the lowest concentration of SAN that resulted in no significant change in OD_{600}.

Effect of SAN on membrane integrity of *E. cloacae*

The integrity of *E. cloacae* cell membranes was assessed by measuring the leakage of intracellular nucleic acids at 260 nm, where UV absorbance is indicative of nucleic acid concentration [14]. TSB media were prepared with SAN concentrations equivalent to the MIC and twice the MIC (2 MIC) identified in previous experiments. *E. cloacae* cultured at 10^8 CFU/mL were inoculated into each medium with a 2% volume fraction. Samples were

collected hourly over a 5-hour, and the absorbance at 260 nm was measured to monitor nucleic acid leakage. Media without SAN were used as control.

Scanning electron microscopy (SEM) analysis

The microstructure of *E. cloacae* cultured with different concentrations of SAN was observed by scanning electron microscopy (SEM). Cultures grown to the logarithmic phase were inoculated with a 2% volume fraction in a media containing the MIC and 2 MIC of SAN, and incubated at 37°C for 24 h. Media without SAN were used as control. Samples were centrifuged at 400 × g for 10 min, washed twice with sterile phosphate buffered saline (PBS), and fixed in 2.5% glutaraldehyde at 4°C overnight. After three times of PBS washes, the bacteria were dehydrated in a graded ethanol series (30, 50, 70, 85, and 95% for 15 min each), and then twice in 100% ethanol for 20 min each. Samples were then freeze-dried and sputtered with gold for SEM (Helios 5 CX, Thermo Fisher Scientific, New York, USA) observation.

Transcriptomic analysis

Based on these findings, we selected two samples from the control and 2 MIC SAN-treated groups for transcriptomic and metabolomic analyses. Total RNA was extracted using the Trizol method. Library preparation and sequencing were conducted by BioMarker Co. Ltd. (China) on the Illumina platform. After obtaining the sequencing data of each sample, fastp software was used to evaluate the data quality of sequencing and remove low-quality data. The quality control conditions were as follows: the mass value of a single base must be greater than 15, the size of the shear slip window must be 4 and the average quality value in the slip window must be greater than 20, and the length of reads after quality control must be greater than 75 bp. High-quality sequences obtained by quality control are used for downstream data analysis. Gene expression levels were quantified using FPKM values, and differential gene expression was analyzed using DESeq 2 software. Differential expressed genes (DEGs) were identified and subjected to GO and KEGG enrichment analyses.

Metabolomics analysis

Metabolite profiling was performed by BioMarke Co. Ltd. (China), using the Waters Acquity I-Class PLUS ultra-high performance liquid tandem Waters Xevo G2-XS QT of high resolution mass spectrometer (LC-QTOF) platform for qualitative and quantitative analyses. Both positive and negative ion modes were utilized in liquid chromatography and mass spectrometry [15]. Metabolomics data were analyzed using the orthogonal projections to latent structures-discriminant analysis (OPLS-DA) model to identify differential metabolites, which were then subjected to GO and KEGG enrichment analyses.

Integrated transcriptomics and metabolomics analysis

To elucidate the mechanisms underlying SAN's effects on *E. cloacae*, DEGs and differential metabolites were analyzed jointly. Heat maps were constructed to visualize the relationship between genes and metabolites, proving a comprehensive overview of the regulatory networks influenced by SAN.

Statistical analyses

Each concentration was repeated three times to ensure consistency. Data were analyzed using SPSS 20. Differences between groups were assessed using one-way ANOVA followed by Duncan's post hoc test. A P-value less than 0.05 was considered statistically significant. Data were presented as the mean ± standard deviation. Graphs were generated using GraphPad Prism 8.0.

Results

In vitro antibacterial activity of SAN against *E. cloacae*

The inhibitory effects of varying concentrations of SAN on *E. cloacae* are depicted in Fig. 1. The minimum inhibitory concentration (MIC) of SAN against *E. cloacae* was determined to be 100 μg/mL, via the broth dilution method. Agar diffusion assays revealed that the inhibition zone increased proportionally with SAN concentration. Specifically, at concentration of 100, 200, 400, and 800 μg/mL, the diameters of the inhibition zones were 10.0, 17.0, 20.5, and 24.0 mm, respectively. These findings indicate a potent, dose-dependent inhibitory effect of SAN on *E. cloacae*.

Effect of SAN on the cell membrane integrity of *E. cloacae*

The integrity of *E. cloacae* cell membranes was initially examined by measuring absorbance at 260 nm, an indicator of nucleic acid leakage. The OD_{260} values of *E. cloacae* are presented in Fig. 2. In the control group, the absorbance at 260 nm remained stable over 5 h, while the absorbance of the experimental group exhibited an increasing trend and showed a significant difference from the control group. Notably, the absorbance in the 2 MIC group was consistently higher than that in the MIC group. This demonstrates that exposure to SAN results in an increase in the leakage of bacterial cell components, which occurs in a dose-dependent manner. This suggests that SAN disrupts cell membrane integrity and permeability, leading to cell rupture and minor leakage of intracellular material.

The effect of SAN on the morphology of *E. cloacae*

The impact of SAN on the cell morphology of *E. cloacae* was examined using SEM. Significant alterations

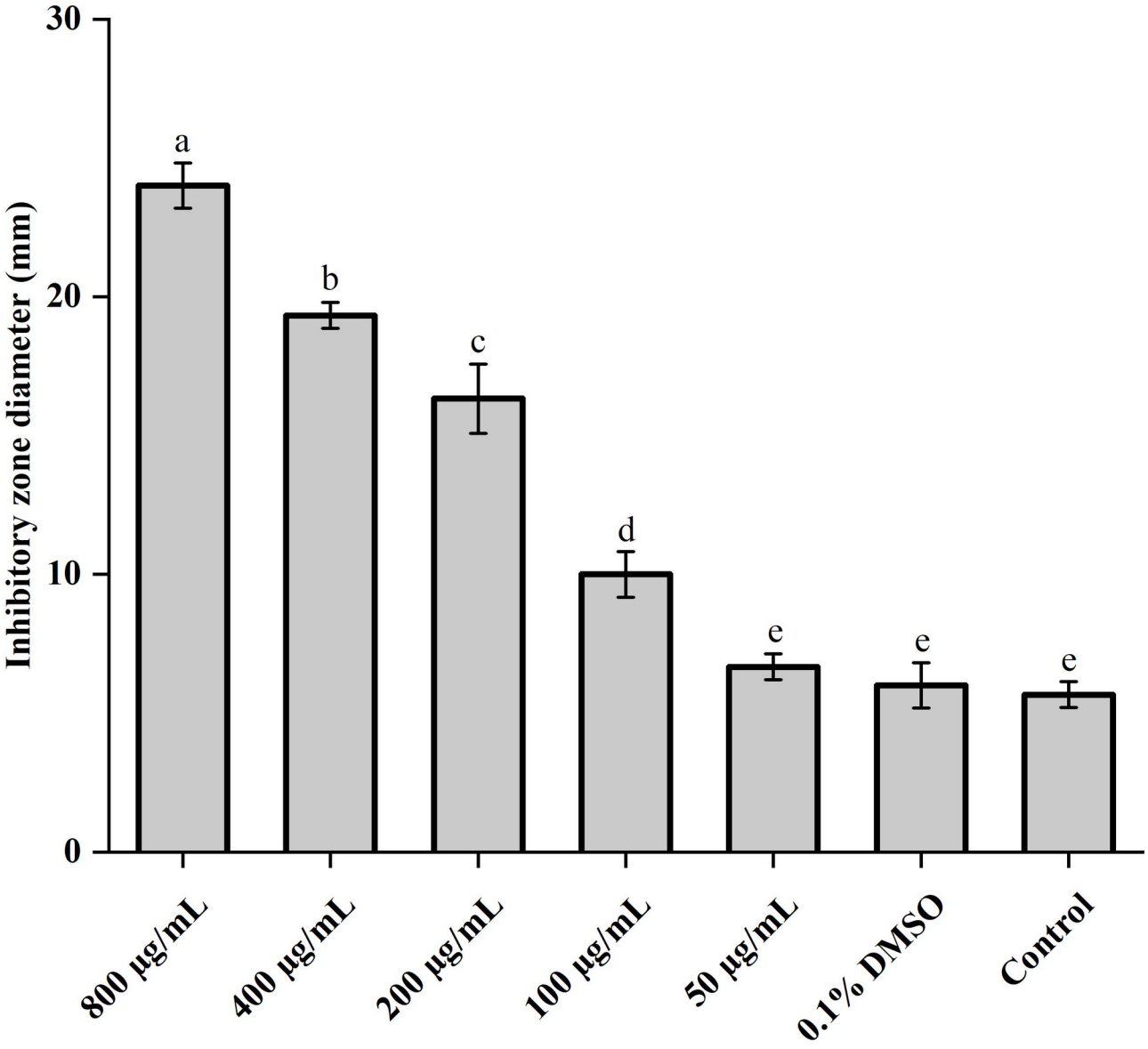

Fig. 1 Inhibitory effect of different concentrations of SAN on *E. cloacae*. The concentration of sanguinarine was 50, 100, 200, 400 and 800 μg/mL, respectively. 0.1% DMSO: Negative control. Control: *E. cloacae* not treated with SAN

in bacterial cell structure were observed, as shown in Fig. 3. The control group exhibited regular, rod-shaped surfaces (Fig. 3A). However, cells treated with the MIC of SAN displayed irregularities, including non-uniform length, elongation, and deformation (Fig. 3B). The 2 MIC treatment group showed evidence of bacterial rupture (Fig. 3C). These findings suggest that SAN can directly causes morphological damage to *E. cloacae*, thereby inhibiting their growth.

Transcriptomic analysis of *E. cloacae* treated with SAN

RNA sequencing of six samples from the control and 2 MIC SAN-treated groups showed high-quality data, with Q20 values near 98% and Q30 values between 93% and 95% (Table S1), which indicated that the quality of the RNA-seq data was superior and could be used for the analysis of the transcriptome. Principal component analysis (PCA) confirmed good reproducibility among experimental samples, with one outlier in the control group (Fig. S1). The differentially expressed genes (DEGs) between the different groups were statistically analyzed, and the distribution of DEGs is shown in a volcano plot (Fig. 4A). The results revealed a total of 406 DEGs between the two groups. Among them, 84 genes were significantly up-regulated and 322 genes were significantly down-regulated (Table S2). It suggested that SAN has a notable impact on the gene expression profile of *E. cloacae*. GO enrichment analysis indicated that the

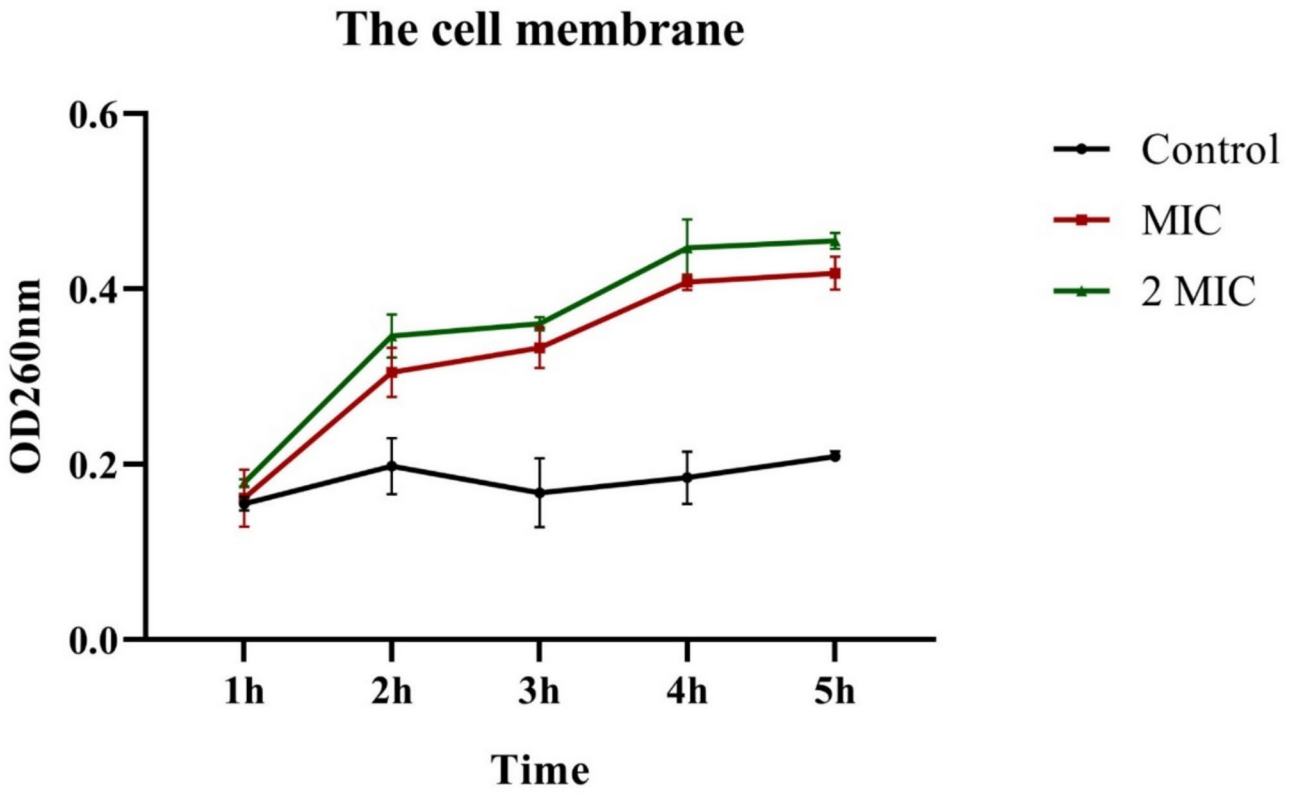

Fig. 2 Effect of SAN on cell membrane permeability in *E. cloacae*. Control: *E. cloacae* not treated with SAN. MIC: *E. cloacae* was incubated treated with MIC of SAN. 2 MIC: *E. cloacae* was incubated treated with 2 MIC of SAN

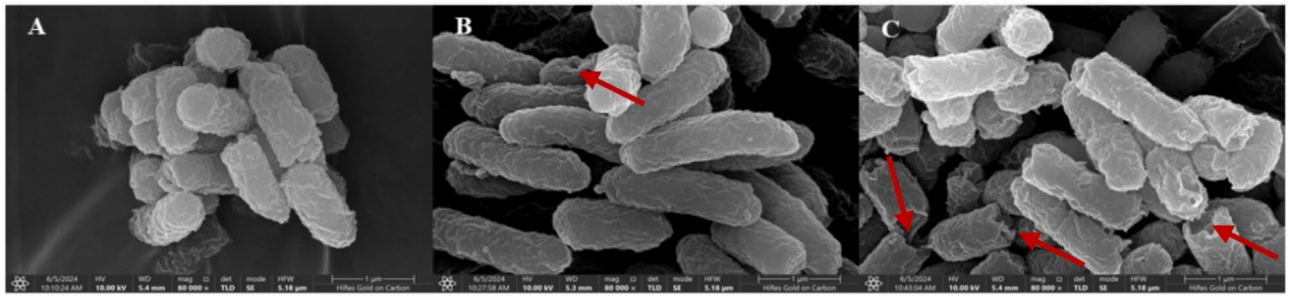

Fig. 3 Scanning electron microscopy of *E. cloacae* after treatments with SAN. Control group (**A**). *E. cloacae* was incubated treated with MIC of SAN (**B**). *E. cloacae* was incubated treated with 2 MIC of SAN (**C**)

DEGs were mainly involved in processes related to cell membranes, transmembrane transport, and ion transport (Fig. 4B). This is consistent with the above findings, which indicate that SAN treatment affects the membrane of *E. cloacae*. KEGG pathway analysis revealed that the DEGs were predominantly enriched in metabolic processes such as amino acid sugar and nucleotide sugar metabolism, arginine and proline metabolism, and pyrimidine metabolism (Fig. 4C). These results indicate that SAN has a notable impact on the gene expression profile of *E. cloacae.*

Effect of SAN on the metabolome of *E. cloacae*

In order to better understand the effect of SAN on *E. cloacae*, a metabolomics analysis was conducted. The metabolic changes following SAN exposure were analyzed using an OPLS-DA model, revealing significant differences between control and treated groups (Fig. 5A). The screening criteria are FC > 1, P value < 0.05 and VIP > 1. A total of 424 differential metabolites (DEMs) were identified, of which 280 were significantly up-regulated and 144 were significantly down-regulated (Table S3). Cluster analysis showed clear separation between metabolites of the control and treated groups (Fig. 5B). The red areas

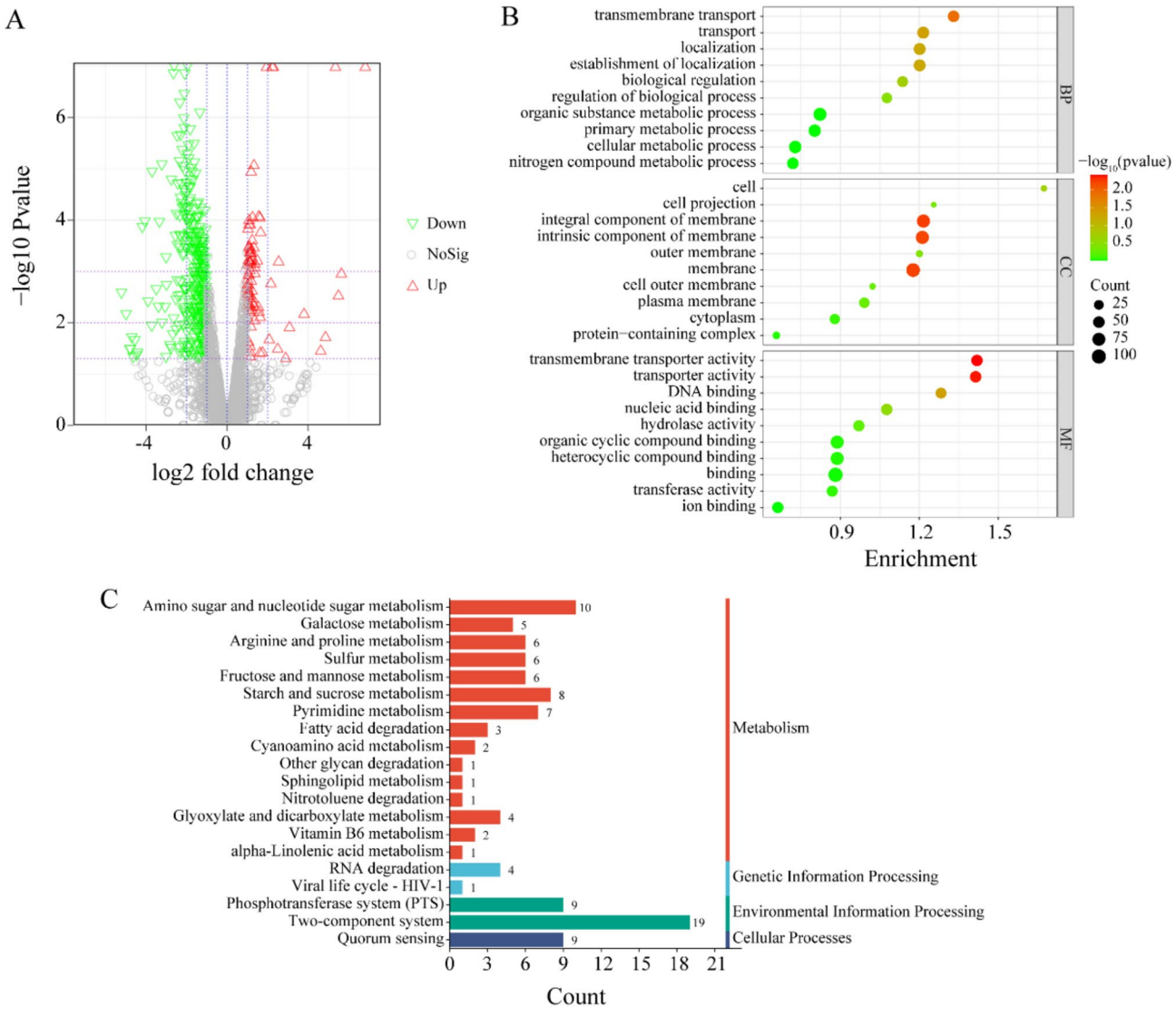

Fig. 4 Transcriptome analysis. The differential gene volcano map. Each triangle in the plot represents a gene, red indicates increased differential expression, green indicates decreased differential expression, and genes without significant differential expression are represented by grey dots (**A**). Bubble diagram of GO enrichment analysis (**B**); KEGG enrichment analysis graph (**C**)

in the heat map represent higher levels of each group of metabolites and the green areas represent lower levels.

DEMs were compared between the 2 MIC SAN group and the control group using a comprehensive metabolic data analysis platform from BMKCloud (www.biocloud.net.). KEGG pathway analysis indicated that SAN treatment disturbed the one carbon pool by folate, amino sugar and nucleotide sugar metabolism, and folate biosynthesis (Fig. 6A). Specifically, folic acid, 7,8-dihydrofolate, and 5,10-methyl-tetrahydrofolate were significantly up-regulated, whereas they were not detected in the control group, leading to a metabolic imbalance in folate biosynthesis (Fig. 6B-C). Thus, SAN can inhibit the growth and reproduction of *E. cloacae* by interfering with folate synthesis. At the same time, SAN disturbed the amino sugar and nucleotide sugar metabolism of *E. cloacae* (Fig. 6D), in which the GDP-N-acetyl-D-per content was significantly down-regulated in this pathway. In addition, glycerophospholipid metabolism was affected, suggesting that the bacterial cell membrane of *E. cloacae* is the target of SAN action (Fig. 6E).

Integrated analysis of the transcriptome and metabolome

In order to gain a comprehensive understanding of the effect of SAN on *E. cloacae*, integrated analysis of the transcriptome and metabolome was performed to reveal the regulatory roles and mechanisms of influence between DEGs and DEMs. KEGG pathway analysis highlighted significant enrichment in amino acid and energy metabolism pathways, including phenylalanine

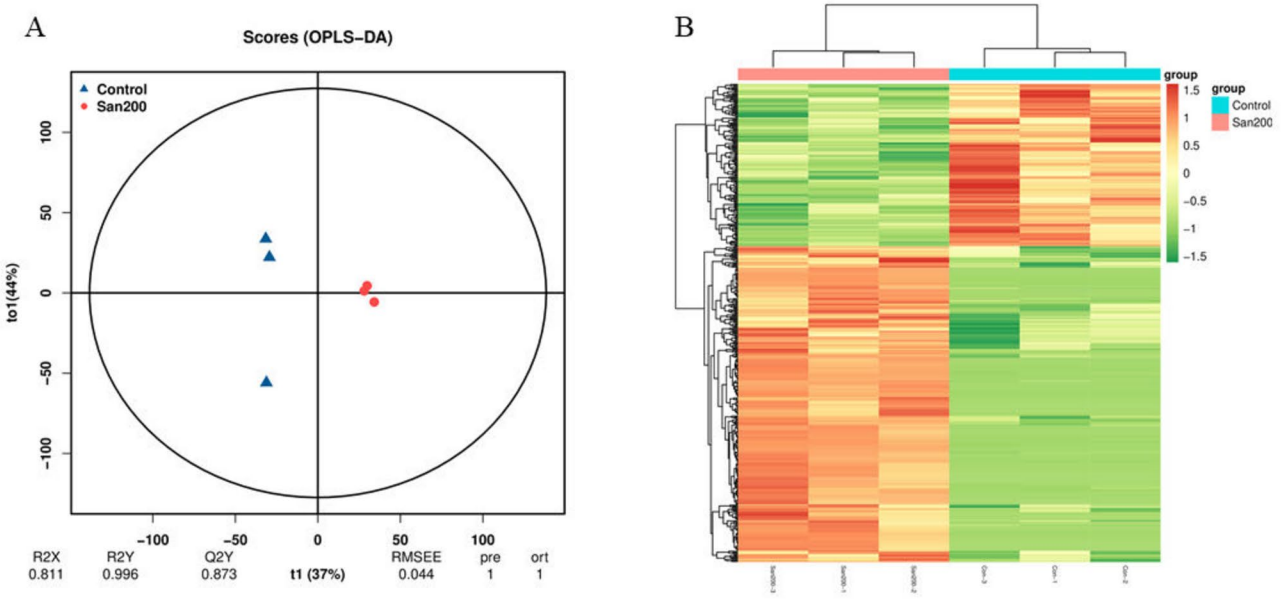

Fig. 5 Differential metabolites produced by SAN against *E. cloacae*. The OPLS-DA plots of the metabolomics data for *E. cloacae* were based on the exposure and control groups (**A**). Clustered heat map analysis of *E. cloacae* metabolites under SAN and control exposure (**B**)

metabolism, tryptophan metabolism, arginine and proline metabolism, glycolysis and citrate cycle (TCA cycle) (Fig. 7A). Correlation analysis between DEGs and DEMs was visualized in a heat map, demonstrating the regulatory interactions influenced by SAN (Fig. 7B).

Discussion

E. cloacae is a conditionally pathogenic bacterium, that has become an increasingly important etiologic agent of hospital-acquired infections, particularly with the widespread use of cephalosporins [16]. SAN, a natural antimicrobial agent derived from plants, exhibits a broad antimicrobial spectrum and notable efficacy [17]. Although SAN has been extensively utilized in pesticides for its insecticidal properties [18], its inhibitory effect on *E. cloacae* has not been well-documented. Our study shows that SAN exhibits potent bacteriostatic activity against *E. cloacae*, with a MIC of 100 μg/mL as determined by microbial colony dilution assays. The antimicrobial activity of SAN against *E. cloacae* was investigated in vitro across various concentrations. The results showed that SAN significantly inhibited the growth of *E. cloacae*, aligning with previous findings that SAN antagonized both Gram-positive [19] and Gram-negative bacteria such as *E. coli* [16]. The bacteria cell membrane is a crucial component that responsible for regulating the transport or diffusion of numerous small molecules and proteins between the interior and exterior of the cell [20]. Previous studies have shown that SAN significantly enhances the permeability and decreases the membrane flux of *Staphylococcus aureus* cell membranes, leading to the dissipation of the membrane potential and bacterial death [21]. In our study, a steady increase in absorbance at 260 nm indicated that SAN disrupted the integrity of the cell membrane of *E. cloacae*. In addition, SEM analysis revealed that cells of SAN-treated *E. cloacae* exhibited elongation and even rupture, consistent with previous observations of morphological changes in bacteria treated with carvacrol oil [13]. These findings confirm that SAN inhibits *E. cloacae* by disrupting cell morphology integrity and morphology.

To elucidate the underlying mechanism of SAN's inhibitory effects on *E. cloacae*, we employed transcriptomic and metabolomic analyses. Transcriptomic analysis revealed significant enrichment of DEGs in pathways related to amino acid sugar and nucleotide sugar metabolism, pyrimidine metabolism, and arginine and proline metabolism. SAN down-regulated the expression of glucokinase (*glk*), a key enzyme in amino acid sugar and nucleotide sugar metabolism, thereby disrupting glucose metabolism and consequently altering energy homeostasis [22]. Additionally, SAN up-regulated the proline utilization A enzyme (*Put A*), which converts proline to glutamate in two successive oxidative steps. Some *Put A* enzymes also function as DNA-binding transcriptional repressors of proline utilization genes [23]. Conversely, *Rut B* was significantly up-regulated; this enzyme plays a crucial role in maintaining normal metabolic activity and bacterial viability, and may also be involved in regulating bacterial virulence and gene expression [24]. Disruption of these metabolic pathways within bacteria can hinder bacterial growth and development, ultimately leading to cell death [25]. The discovery of non-targeted intracellular metabolites was used to identify key metabolic

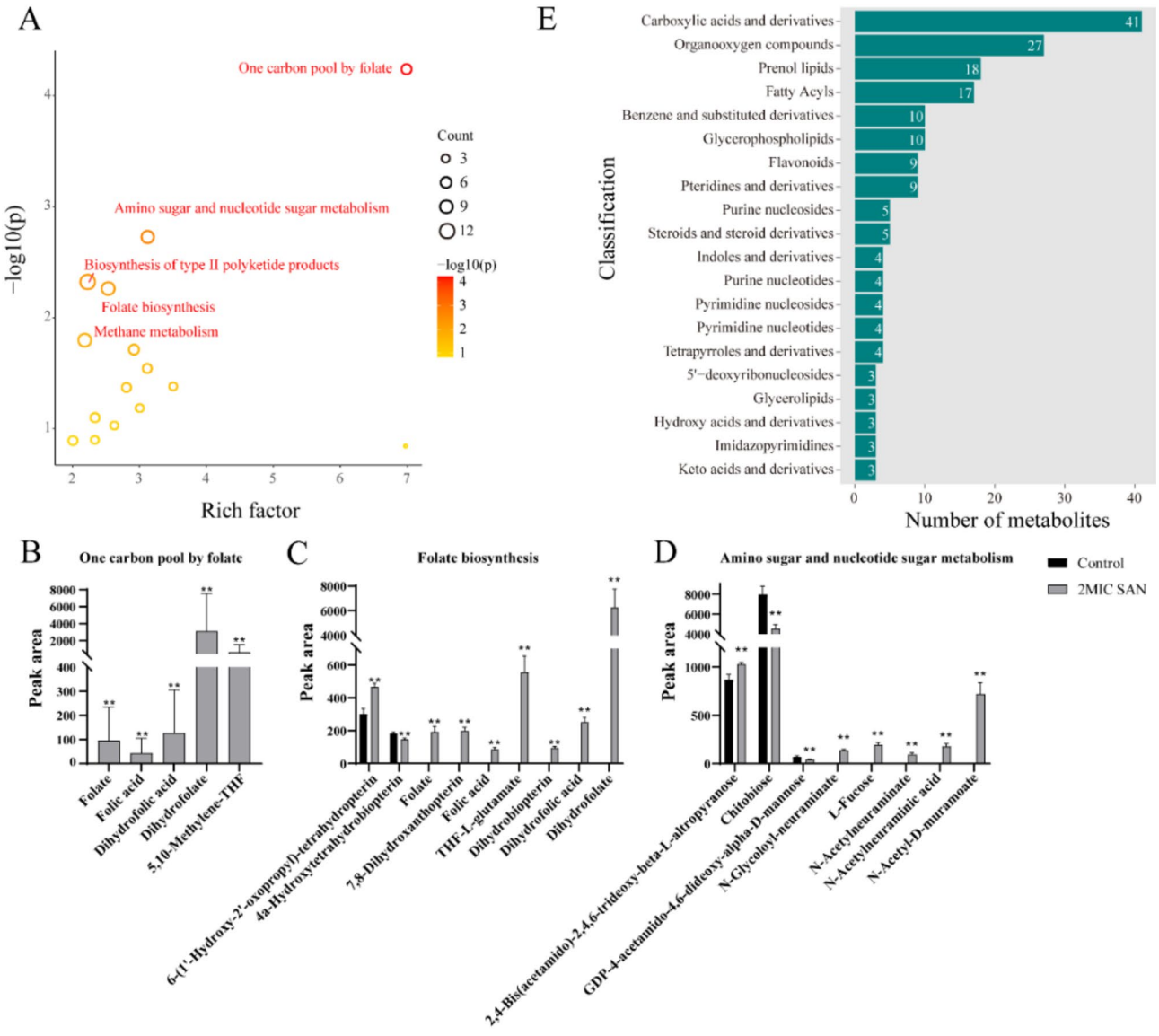

Fig. 6 Metabolomics KEGG enrichment analysis. Bubble plots showing differential metabolic compound pathway enrichment analysis under control and SAN exposure to 2 MIC (**A**). Changes in metabolite biomarkers in one carbon pool by folate, folate biosynthesis, and amino sugar and nucleotide sugar metabolism pathways (**B**, **C**, and **D**). *$p < 0.05$, **$p < 0.01$ ((by comparison with control Student t-test). Plot of differential metabolite categorization (**E**)

pathways that lead to bacterial death and to reveal mechanisms of bacterial inhibition [26]. Analysis of metabolomics revealed that differential metabolites were mainly involved in one carbon pool by folate, amino sugar and nucleotide sugar metabolism, and folate biosynthesis. Folic acid is an essential metabolite for numerous carbon transfer reactions and serves as a key precursor for the synthesis of purines, pyrimidines, and amino acids [27]. Bacteria must synthesize folate de novo, as they cannot uptake it from the environment [28]. Folate synthesis relies on three primary precursors: Guanosine 5-triphosphate (GTP), Para-Aminobenzoic Acid (PABA), and glutamate [29]. GTP also serves as a precursor for riboflavin synthesis. In this experiment, the expression of the key pathway gene *purN* was down-regulated, resulting in an insufficient supply of GTP, which affects the folate synthesis, thereby inhibits the growth and reproduction of *Enterobacter cloacae* [27]. Nucleotides are critical components of peptidoglycan, which is essential for normal bacterial growth and division [30]. Peptidoglycan is a component of cell wall glycans and plays an invaluable role in maintaining bacterial cell morphology and resisting osmotic pressure [31]. Amino sugar and nucleotide sugar metabolism are strongly associated with the growth and development of organisms [32]. Following Sanguinarine treatment, we observed up-regulation of peptidoglycan biosynthesis-related genes *murB*, *murE*, and *murF*. Among them, UDP-N-acetylglucosamine reductase,

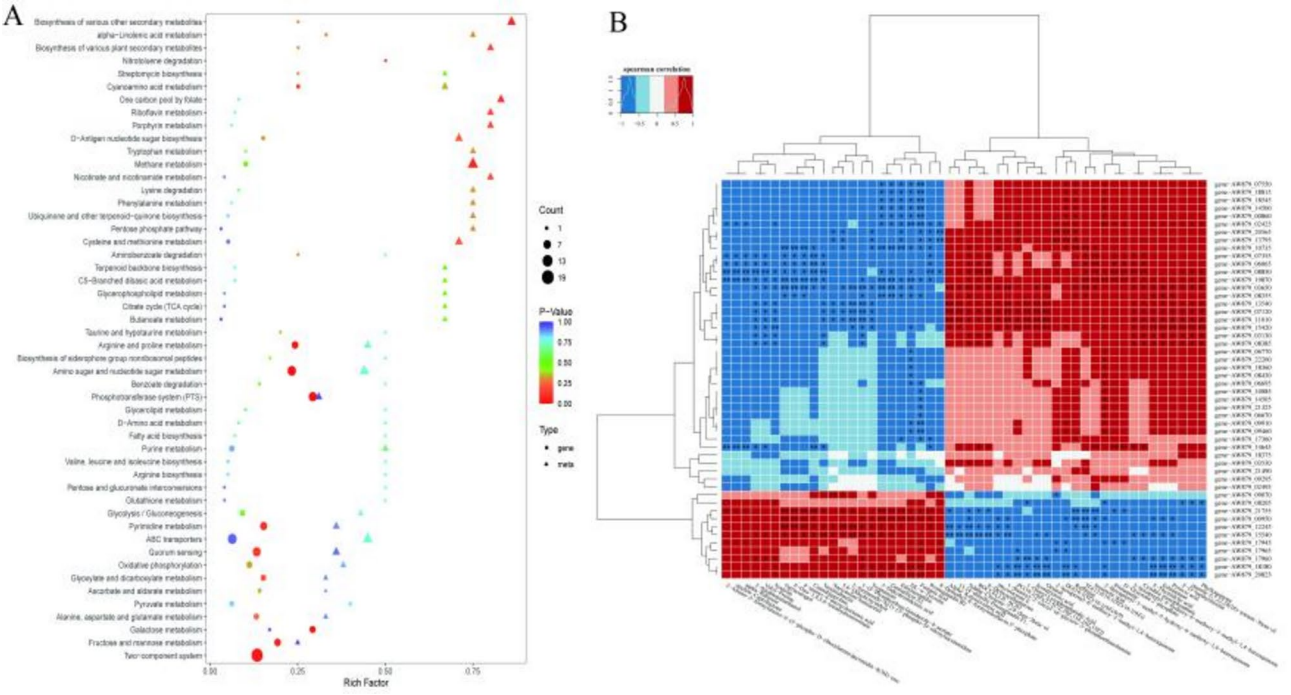

Fig. 7 Integrated analysis of the transcriptome and metabolome. Bubble diagram of differential metabolite and differential gene enrichment analysis (**A**). The dots represent genes and the triangles represent metabolites; the size of the bubbles represents the number of differential metabolites or genes, with the larger the number, the larger the dot. Heatmap of correlation clustering between metabolites and genes (**B**). Color shades indicate the size of correlation, blue indicates negative correlation, red indicates positive correlation, p-value is the result of correlation test, * in the graph indicates $p \leq 0.05$, ** indicates $p \leq 0.01$

which is encoded by the *MurB*, catalyzes the second key step in peptidoglycan biosynthesis. These results suggest that SAN discrupts cell wall integrity by inhibiting peptidoglycan synthesis.

In the joint transcriptome and metabolome analysis experiments, we observed significant down-regulation of tryptophan, phenylalanine, arginine, and proline, along with their associated genes, including *dad A*, *ipdG*, *Put A*, *astA*, and *proC*. Tryptophan is a precursor for many key biomolecules as it plays a central role in diverse metabolic pathways in organisms [33]. Indoles are key secondary compounds that derived from tryptophan [34]. The *ipdG* gene encodes indole pyruvate decarboxylase, an enzyme that catalyzes the decarboxylation of tryptophan to indole pyruvate, a critical step in the indole pathway [35]. The reduced indole content in *E. cloacae* following SAN treatment may affect their growth and metabolism directly. Phenylalanine plays an essential role in cellular metabolism, ligand recognition and protein synthesis, and the production of a wide range of biologically active molecules [36]. The *dadA* gene is critical in phenylalanine metabolism, primarily involved in its synthesis and regulation [37]. The *dadA* gene encodes for enzymes that are involved in a key step in the synthesis of phenylalanine that is essential for the maintenance of cellular levels of phenylalanine [37]. Down-regulation of *dadA* directly affects the rate and amount of phenylalanine synthesis. Arginine and proline are not only essential protein stabilizers and osmoregulators, but also involved in the synthesis of creatine from methionine [38]. In addition, arginine and proline can be converted to glutamate to produce glutathione which in turn plays a role in maintaining redox balance and preventing oxidative stress [36]. Thus, arginine and proline metabolism is crucial for bacterial growth and reproduction [39]. Glycolysis and the TCA cycle are main pathways that provide energy to the body [40]. In this study, SAN down-regulated the genes involved in glycolysis, such as *glk*, *crr*, *ptsG* and *malX*, which mainly affect the glucose transport and metabolism process, resulting in the down-regulation of pyruvate. Pyruvate is not only the end product of glycolysis, but also the hub connecting glycolysis and the TCA cycle [36]. As a key reactant of the TCA cycle, the down-regulation of pyruvate results in the entire TCA cycle receiving inhibition, resulting in an inadequate energy supply, which ultimately caused bacterial dysfunction and death.

Conclusion

This study systematically analyzed the inhibitory effect of SAN on *E. cloacae* and its underlying mechanism using integrated transcriptomics and metabolomics

approaches. SAN exhibited strong antibacterial activity against *E. cloacae*, which can effectively inhibit its growth and disrupt its bacterial morphology. Comprehensive metabolomics and transcriptomics analyses revealed that SAN affects the growth of *E. cloacae* by inhibiting amino acid synthesis and energy metabolism processes. These findings suggest that SAN exerts its antibacterial effect through multiple pathways, providing a potential therapeutic agent for human diseases, an alternative to plant and animal antibiotics, and a biopesticide. This study lays a theoretical foundation for the application of SAN as a new natural antimicrobial agent for the prevention and treatment of *E. cloacae* infections.

Supplementary Information

The online version contains supplementary material available at https://doi.org/10.1186/s12866-025-03992-8.

Supplementary Material 4: Figure S1: PCA plots of the transcriptomes of the control and experimental groups.

Supplementary Material 1: Table S1: Statistical analysis of RNA seq data quality.

Supplementary Material 2: Table S2: Differential genes.

Supplementary Material 3: Table S3: Differential metabolites.

Author contributions

Ting Yang: Writing - original draft, Software, Data curation. Haojie Sha: Grammar revision. Wenlu Bi: revise the manuscript. Jianguo Zeng: Review and validation. Dingding Su: Methodology, Data curation, revise the manuscript, Project administration.

Funding

This study was supported by the Taishan Industrial Experts Program and the Yuandu Industry Leading Talents Project.

Data availability

All data supporting the findings of this study are available within the paper and its Supplementary Information.

Declarations

Ethics approval

Not applicable.

Consent for publication

Not applicable.

Competing interests

The authors declare no competing interests.

Received: 12 December 2024 / Accepted: 23 April 2025
Published online: 06 May 2025

References

1. Gao X, Zhou Y, Zhu X, Tang H, Li X, Jiang Q, Wei W, Zhang X. Enterobacter cloacae: A probable etiological agent associated with slow growth in the giant freshwater Prawn Macrobrachium rosenbergii. Aquaculture. 2021;530:735826.
2. Jin M, Zheng L, Wei Y, Cheng J, Zhang D, Yan S, Qin H, Wang Q, Ci X, Feng H. Enterobacter cloacae aggravates metabolic disease by inducing inflammation and lipid accumulation. Environ Toxicol Phar. 2022;90:103819.
3. Mabrok M, Algammal AM, El-Tarabili RM, Dessouki AA, ElBanna NI, Abd-Elnaby M, El-Lamie MMM, Rodkhum C. Enterobacter cloacae as a re-emerging pathogen affecting mullets (Mugil spp.): pathogenicity testing, LD50, antibiogram, and encoded antimicrobial resistance genes. Aquaculture. 2024;583:740619.
4. Choi WJ, Dong HJ, Jeong HU, Jung HH, Kim YH, Kim TH. Antiobesity effects of Lactobacillus plantarum LMT1-48 accompanied by Inhibition of Enterobacter cloacae in the intestine of Diet-Induced obese mice. J Med Food. 2019;22(6):560–6.
5. Carrillo-Hormaza L, Mora C, Alvarez R, Alzate F, Osorio E. Chemical composition and antibacterial activity against Enterobacter cloacae of essential oils from Asteraceae species growing in the páramos of Colombia. Ind Crop Prod. 2015;77:108–15.
6. Liu J, Xu Z, Guo Z, Zhao Z, Zhao Y, Wang X. Structural investigation of a polysaccharide from the mycelium of Enterobacter cloacae and its antibacterial activity against extensively drug-resistant E. cloacae producing SHV-12 extended-spectrum β-lactamase. Carbohyd Polym. 2018;195:444–52.
7. Liu W, Su E. Screening, evaluation and identification of promising plant extracts for development of novel natural preservatives. Food Biosci 2024:103672.
8. Huang L-J, Lan J-X, Wang J-H, Huang H, Lu K, Zhou Z-N, Xin S-Y, Zhang Z-Y, Wang J-Y, Dai P, et al. Bioactivity and mechanism of action of sanguinarine and its derivatives in the past 10 years. Biomed Pharmacother. 2024;173:116406.
9. Galadari S, Rahman A, Pallichankandy S, Thayyullathil F. Molecular targets and anticancer potential of sanguinarine—a benzophenanthridine alkaloid. Phytomedicine. 2017;34:143–53.
10. Zhang L, Ma L, Yang Q, Liu Y, Ai X, Dong J. Sanguinarine protects channel catfish against Aeromonas hydrophila infection by inhibiting Aerolysin and biofilm formation. Pathogens (Basel Switzerland) 2022; 11(3).
11. Bavarsadi M, Mahdavi AH, Ansari-Mahyari S, Jahanian E. Sanguinarine improved nutrient digestibility, hepatic health indices and productive performance in laying hens fed low crude protein diets. Veterinary Med Sci. 2021;7(3):800–11.
12. Lin Y, Tang X, Xu L, Wang S. Antibacterial properties and possible action mechanism of chelating peptides-zinc nanocomposite against Escherichia coli. Food Control. 2019;106:106675.
13. Gutierrez-Pacheco MM, Gonzalez-Aguilar GA, Martinez-Tellez MA, Lizardi-Mendoza J, Madera-Santana TJ, Bernal-Mercado AT, Vazquez-Armenta FJ, Ayala-Zavala JF. Carvacrol inhibits biofilm formation and production of extracellular polymeric substances of Pectobacterium carotovorum subsp. carotovorum. Food Control. 2018;89:210–8.
14. Song Y, Ren Y, Xue Y, Lu D, Yan T, He J. Putrescine (1,4-Diaminobutane) enhances antifungal activity in postharvest Mango fruit against Colletotrichum gloeosporioides through direct fungicidal and induced resistance mechanisms. Pestic Biochem Phys. 2023;195:105581.
15. Zhang S, Lu X, Hu C, Li Y, Yang H, Yan H, Fan J, Xu G, Abnet CC, Qiao Y. Serum metabolomics for biomarker screening of esophageal squamous cell carcinoma and esophageal squamous dysplasia using gas Chromatography-Mass spectrometry. Acs Omega. 2020;5(41):26402–12.
16. Panigrahi S, Rath CC. In vitro characterization of antimicrobial activity of an endophytic bacterium Enterobacter cloacae (MG001451) isolated from Ocimum sanctum. S Afr J Bot. 2021;143:90–6.
17. Liang J, Li X, Bi C, Yu Y, Liu W, Zhang X, Cao W. Sanguinarine, similar to the mics of spectinomycin, exhibits good anti-Neisseria gonorrhoeae activity in vitro. J Infect Chemother. 2023;29(9):927–9.
18. Duan P, Wei M, Li M, Gao L. The allelopathic algicides sanguinarine and Berberine reduced the dominance of Microcystis in competition with Chlorella. Results Eng. 2022;16:100714.
19. Hamoud R, Reichling J, Wink M. Synergistic antibacterial activity of the combination of the alkaloid sanguinarine with EDTA and the antibiotic streptomycin against multidrug resistant bacteria. J Pharm Pharmacol. 2015;67(2):264–73.
20. Zhang Q, Lyu Y, Huang J, Zhang X, Yu N, Wen Z, Chen S. Antibacterial activity and mechanism of sanguinarine against Providencia rettgeri in vitro. Peerj. 2020;8:e9543.
21. Gu Y, Dong J, Li J, Luo Q, Dong X, Tang G, Zhang J, Du X, Pu Q, He L, et al. Antibacterial activity and mechanism of sanguinarine against Staphylococcus aureus by interfering with the permeability of the cell wall and membrane and inducing bacterial ROS production. Front Veterinary Sci. 2023;10:1121082.

22. He R, Wei P, Odiba AS, Gao L, Usman S, Gong X, Wang B, Wang L, Jin C, Lu G, et al. Amino sugars influence Aspergillus fumigatus cell wall polysaccharide biosynthesis, and biofilm formation through interfering Galactosaminogalactan deacetylation. Carbohyd Polym. 2024;324:121511.
23. Liu LK, Becker DF, Tanner JJ. Structure, function, and mechanism of proline utilization A (PutA). Arch Biochem Biophys. 2017;632:142–57.
24. Vogels GD, Van der Drift C. Degradation of purines and pyrimidines by microorganisms. Bacteriological Reviews. 1976;40(2):403–68.
25. Xiong S, Xu X, Liu Q, Xu Y, Ren H, Xiong T, Xie M. Integrated metatranscriptomics and metabolomics revealed the metabolic pathways of biogenic amines during Laotan suancai fermentation. Food Biosci. 2024;57:103517.
26. Zheng X, Al Naggar Y, Wu Y, Liu D, Hu Y, Wang K, Jin X, Peng W. Untargeted metabolomics description of propolis's in vitro antibacterial mechanisms against Clostridium perfringens. Food Chem. 2023;406:135061.
27. Yang H, Zhang X, Liu Y, Liu L, Li J, Du G, Chen J. Synthetic biology-driven microbial production of folates: advances and perspectives. Bioresource Technol. 2021;324:124624.
28. Wang Y, Jin Y, Wang Y, Li L, Liao Y, Zhang Y, Yu D. The effect of folic acid in patients with cardiovascular disease: A systematic review and meta-analysis. Medicine. 2019;98(37):e17095.
29. Du H, Hu Y, Lu K, Li T, Tian Y, Hu Y. Potential folate-producing strains and their applications in biofortification of fermented Moringa oleifera leaves powder. LWT. 2023;187:115357.
30. Tucker SA, Hu S-H, Vyas S, Park A, Joshi S, Inal A, Lam T, Tan E, Haigis KM, Haigis MC. SIRT4 loss reprograms intestinal nucleotide metabolism to support proliferation following perturbation of homeostasis. Cell Rep. 2024;43(4):113975.
31. Sun Y, Yuan X, Luo Z, Cao Y, Liu S, Liu Y. Metabolomic and transcriptomic analyses reveal comparisons against liquid-state fermentation of primary dark tea, green tea and white tea by Aspergillus cristatus. Food Res Int. 2023;172:113115.
32. Lin X-L, Guo F, Rillig MC, Chen C, Duan G-L, Zhu Y-G. Effects of common artificial sweeteners at environmentally relevant concentrations on soil springtails and their gut microbiota. Environ Int. 2024;185:108496.
33. Liu X-h. Zhai X-y. Role of Tryptophan metabolism in cancers and therapeutic implications. Biochimie. 2021;182:131–9.
34. Henson JM, Butler MJ, Day AW, THE DARK SIDE OF. THE MYCELIUM: melanins of phytopathogenic Fungi. Annu Rev Phytopathol. 1999;37:447–71.
35. Le Floc'h N, Otten W, Merlot E. Tryptophan metabolism, from nutrition to potential therapeutic applications. Amino Acids. 2011;41(5):1195–205.
36. Liang T, Wang X, Chen L, Ding L, Wu J, Zhang J, Wang R. Transcriptomic and metabolomic analyses reveal the antibacterial mechanism of Zanthoxylum bungeanum Maxim. Essential oil against GBS. Food Biosci. 2024;57:103528.
37. Belodel AV, Paramonov DA, Korovina MV, Muliashov SA, Markvichev NS. [Bioconversion of phenyllactate to phenylalanine by bacteria of the genus Pseudomonas]. Prikl Biokhim Mikrobiol. 2005;41(1):48–52.
38. Yuan H, Xu Y, Chen Y, Zhan Y, Wei X, Li L, Wang D, He P, Li S, Chen S. Metabolomics analysis reveals global acetoin stress response of Bacillus licheniformis. Metabolomics: Official J Metabolomic Soc. 2019;15(3):25.
39. Wang G, Zhang J, Wang G, Fan X, Sun X, Qin H, Xu N, Zhong M, Qiao Z, Tang Y, et al. Proline responding1 plays a critical role in regulating general protein synthesis and the cell cycle in maize. Plant Cell. 2014;26(6):2582–600.
40. Liu M, Feng M, Yang K, Cao Y, Zhang J, Xu J, Hernández SH, Wei X, Fan M. Transcriptomic and metabolomic analyses reveal antibacterial mechanism of astringent persimmon tannin against Methicillin-resistant Staphylococcus aureus isolated from pork. Food Chem. 2020;309:125692.

Publisher's note